Dermatol Ther (Heidelb)
https://doi.org/10.1007/s13555-024-01298-7

ORIGINAL RESEARCH

Evaluation of the Biological Effect of a Nicotinamide-Containing Broad-Spectrum Sunscreen on Photodamaged Skin

Teresa Torres-Moral · Gemma Tell-Martí · Jaume Bague · Pau Rosés-Gibert · Neus Calbet-Llopart · Judit Mateu · Javiera Pérez-Anker · Míriam Potrony · Beatriz Alejo · Pablo Iglesias · Natalia Espinosa · Carmen Orte Cano · Elisa Cinotti · Véronique Del Marmol · Margot Fontaine · Makiko Miyamoto · Jilliana Monnier · Jean Luc Perrot · Pietro Rubegni · Linda Tognetti · Mariano Suppa · Anne Laure Demessant-Flavigny · Caroline Le Floc'h · Leonor Prieto · Josep Malvehy · Susana Puig

Received: June 17, 2024 / Accepted: October 15, 2024

ABSTRACT

***Introduction*:** UVA-UVB increases skin matrix metalloproteinases and breaks down extracellular proteins and fibrillar type 1 collagen, leading to photodamage. Topical application of nicotinamide prevents UV-induced immunosuppression. Several studies have demonstrated the importance of protection against UV. This study aims to determine the biological effect of a high broad-spectrum UVB-UVA sunscreen containing nicotinamide and panthenol (SSNP) on photodamaged skin using linear confocal optical coherence tomography (LC-OCT), immunohistochemistry, and RNA profiling.

***Methods*:** Two areas of severely photodamaged forearm skin (L01 and L02) and one less sun-damaged (naturally protected) area on the inner part of the forearm (L03) were identified in 14 subjects. These areas were imaged using LC-OCT and L01 and L03 were biopsied at baseline. After 4 weeks of treatment with SSNP, L02 was reimaged using LC-OCT, and biopsied. Histology, immunostaining with p21, p53, PCNA, and CPD, and RNA sequencing were performed in all samples.

***Results*:** LC-OCT analysis showed that epidermis thickness and the number of keratinocytes is higher in the sun-exposed areas than in the

Prior Presentation: Data from this work has been partially shown in three previous congresses: (a) Puig S, et al. (2021). Evaluation of the biological effect of a high broad-spectrum sunscreen with nicotinamide and panthenol repairing photodamaged skin. Paper presented at the 19th Congress of the European Society for Photobiology, 30 August–3 September 2021, World Wide Web and Salzburg, Austria. (b) L'Oréal Dermatological Beauty. (2022). Evaluation of the biological effect of a high broad-spectrum sunscreen with nicotinamide and panthenol repairing photodamaged skin. Retrieved from the L'Oréal Dermatological Beauty website. (c) Puig S, et al. (2022). Evaluation of the biological effect of a high broad-spectrum sunscreen with nicotinamide and panthenol repairing photodamaged skin. European Medical Journal. Retrieved from the EMJ Reviews website: www.emjreviews.com.

Supplementary Information The online version contains supplementary material available at https://doi.org/10.1007/s13555-024-01298-7.

T. Torres-Moral · G. Tell-Martí · N. Calbet-Llopart · M. Potrony · J. Malvehy · S. Puig
Centro de Investigación Biomédica en Red de Enfermedades Raras, CIBERER, Instituto de Salud Carlos III, Barcelona, Spain

T. Torres-Moral · G. Tell-Martí · J. Bague · P. Rosés-Gibert · N. Calbet-Llopart · J. Mateu · J. Pérez-Anker · B. Alejo · P. Iglesias · J. Malvehy · S. Puig (✉)
Dermatology Department, Hospital Clínic de Barcelona, IDIBAPS, Villarroel 170, 08036 Barcelona, Spain
e-mail: spuig@clinic.cat; susipuig@ub.edu

J. Pérez-Anker · J. Malvehy · S. Puig

Published online: 07 November 2024

non-exposed areas. Comparing before and after treatment, even though there is a trend towards normalization, the differences were not statistically significant. The expression of p21, PCNA, p53, and CPD increased in severely photodamaged skin compared to less-damaged skin. When comparing before and after treatment, only p21 showed a trend to decrease expression. RNA sequencing analysis identified 1552 significant genes correlating with the progression from non-visibly photodamaged skin to post-treatment and pre-treatment samples; in the analysis comparing pre- and post-treatment samples, 5429 genes were found to be significantly associated. A total of 1115 genes are common in these two analyses. Additionally, nine significant genes from the first analysis and eight from the second are related to collagen. Six of these collagen genes are common in the two analyses. MAPK and cGMP-PKG signalling pathways are upregulated in the progression to photodamage analysis. In the pre- and post-treatment analysis, 32 pathways are downregulated after treatment, the most statistically significant being the ErbB, Hippo, NOD-like receptor, TNF, and NF-kB signalling pathways.
***Conclusion*:** This study demonstrates the role of SSNP in collagen generation, highlights the relevance of the cGMP-PKG and MAPK signalling pathways in photodamage, and shows the ability of SSNP to downregulate pathways activated by UV exposure. Additionally, it deepens our understanding of the effect of SSNP on immune-related pathways.

Universitat de Barcelona, Villarroel 170, 08036 Barcelona, Spain

M. Potrony · N. Espinosa
Biochemistry and Molecular Genetics Department, Hospital Clínic de Barcelona, IDIBAPS, Barcelona, Spain

C. Orte Cano · V. Del Marmol · M. Fontaine · M. Miyamoto · M. Suppa
Dermatology Department, Hôpital Erasme, Université Libre de Bruxelles, Brussels, Belgium

E. Cinotti · P. Rubegni · L. Tognetti
Dermatology Unit, Department of Medical, Surgical and Neurological Sciences, University of Siena, Siena, Italy

J. Monnier
Dermatology and Skin Cancers Department, La Timone Hospital, AP-HM, Aix-Marseille University, Marseille, France

PLAIN LANGUAGE SUMMARY

This study focuses on the damage that sun exposure can do to our skin, also called photodamage. This damage is mainly caused by ultraviolet radiation, which can lead to problems such as wrinkles, changes in skin color, and sagging skin. Nicotinamide, a form of vitamin B_3, helps our cells repair their DNA and prevents them from dying. Previous studies in mice have shown that nicotinamide can protect the immune system against photodamage and reduce the risk of cancer. In order to understand how sunscreen containing nicotinamide and panthenol affects photodamage, an international team of researchers gathered 14 Catalan participants and examined severely sun-damaged skin areas and less sun-damaged skin. We conducted imaging, molecular, and genetic experiments before and after 4 weeks of nicotinamide sunscreen use. The results show that severely sun-damaged skin is thicker and contains more cells called keratinocytes. Additionally, certain indicators of DNA damage and repair are more active in severely sun-damaged skin. Genetic analyses reveal that the photodamage process causes significant differences in certain genetic pathways such as cGMP-PKG and MAPK pathways. Using nicotinamide sunscreen leads to positive changes in several cellular processes, including the way cells divide, respond to stress, and produce collagen. In summary, this study gives us a deeper understanding of skin photodamage and underlines the potential benefits of adding nicotinamide to sunscreens, which could be a promising way to reduce the damage caused by UV radiation.

J. L. Perrot
Melanoma Unit, University Hospital of Saint-Etienne, Saint-Etienne, France

M. Suppa
Dermatology Department, Institut Jules Bordet, Universite Libre de Bruxelles, Brussels, Belgium

A. L. Demessant-Flavigny · C. Le Floc'h
Laboratoire Dermatologique, La Roche-Posay, Levallois-Perret, France

L. Prieto
Scientific Direction, Laboratoire Dermatologique La Roche-Posay, L'Oréal Cosmética Activa, Madrid, Spain

Graphical Abstract:

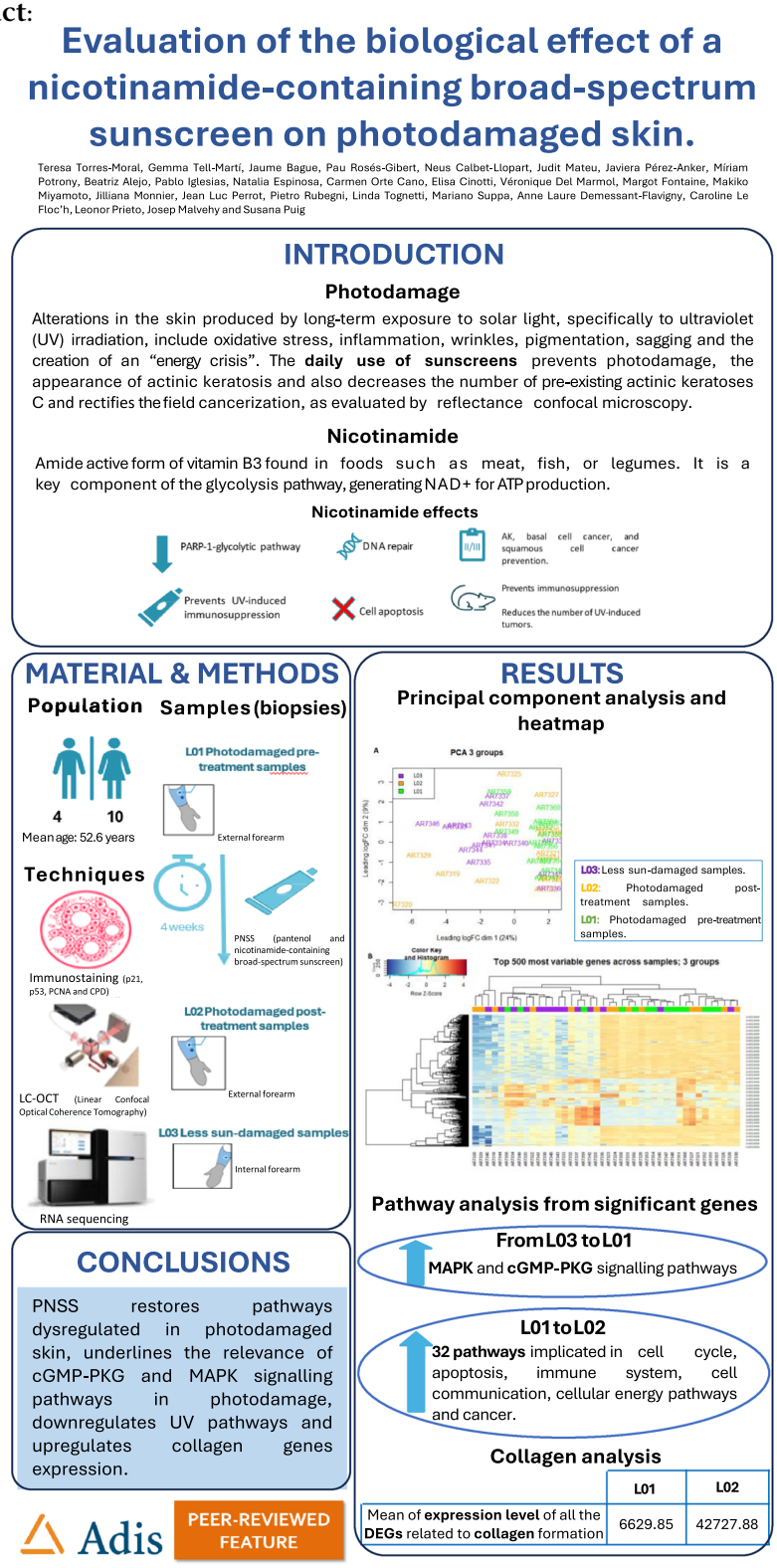

The graphical abstract represents the opinions of the authors. For a full list of declarations, including funding and author disclosure statements, and copyright information, please see the full text online.

Keywords: Collagen; Nicotinamide; Photodamage

Key Summary Points
UVA-UVB increases skin matrix metalloproteinases, leading to photodamage.
Topical application of high broad-spectrum UVB-UVA sunscreen containing nicotinamide and panthenol (SSNP) prevents UV-induced immunosuppression.
SSNP demonstrates proficiency in mitigating UV-triggered pathways and can effectively rectify disrupted pathways affected by photodamage.
SSNP boosts collagen gene expression, aiding photodamage recovery.
cGMP-PKG and MAPK pathways are implicated in the effects of SSNP on photodamaged skin.

DIGITAL FEATURES

This article is published with digital features, including a graphical abstract, to facilitate understanding of the article. To view digital features for this article, go to https://doi.org/10.6084/m9.figshare.26954164.

INTRODUCTION

Skin is crucial in providing protection from exogenous aggression by pathogenic pollutants. Long-term exposure to solar light, specifically ultraviolet (UV) radiation, induces damage to the skin and DNA, provoking oxidative stress and pro-inflammatory cytokine release. This photodamage is mainly evidenced by wrinkles, pigmentation changes, and sagging [1].

UV radiation consists of wavelengths from 200 to 400 nm and is divided into three parts: UVA (320–400 nm), UVB (280–320 nm), and UVC (100–280 nm). Only UVA and UVB reach the earth since the ozone layer shields against UVC [2]. Both UVA and UVB have biological effects on the skin, causing mutations and immunosuppressive effects that contribute to photocarcinogenesis [3, 4]. UVA represents most of the UV rays, whereas UVB, more biologically dangerous, are mutagenic per se and induce cyclobutane pyrimidine dimers (CPD) within the DNA of epidermal cells.

At the dermal layer, mainly UVA, but also UVB, leads to structural and functional changes such as an increase in matrix metalloproteinases and the breakdown of extracellular proteins and fibrillar type 1 collagen.

AP1 is a transcription factor which plays a dominant role in the transcriptional activation of matrix metalloproteinase promoters. It is produced through the UV-generated activation of MAPK pathways, composed of ERK, JNK, and p38. Phosphorylated ERK plays an important role in the trigger for Fos induction, whereas phosphorylated JNK and p38 promote phosphorylation of Jun. Phosphorylated Jun combines with Fos to form a heterodimer, AP1, which binds to target the gene promoters matrix metalloproteinases [5]. Another important matrix metalloproteinase transcription factor is NF-kB, located in the cytoplasm, resulting in translocation of the nucleus by UVB irradiation. Translocated NF-κB increases pro-inflammatory cytokines such as tumor necrosis factor (TNF), interleukin-6 (IL-6), and interleukin-1β (IL-1β), contributing to skin damage [5].

UVB also affects the TGFβ/Smad pathway, a collagen synthesis pathway. Transforming growth factor-β (TGFβ) stimulates the biosynthesis of type 1 collagen and regulates collagen homeostasis through Smad signalling molecules. Reactive oxygen species (ROS) produced by UV irradiation damage the TGFβ signalling pathway by reducing TGFβ receptor II expression and downregulating Smad3 phosphorylation. UVB-induced TGFβ/Smad pathway damage is one of the mechanisms causing loss of collagen [6].

Nicotinamide is an amide active form of vitamin B_3 and a precursor of nicotinamide adenine dinucleotide (NAD). Nicotinamide is metabolized by the liver to NAD, a key component of the glycolysis pathway, generating NAD^+ for ATP production. Nicotinamide increases DNA repair and prevents cell apoptosis [7, 8].

Recent in vitro results suggest that keratinocytes isolated from subjects with field cancerization might be more sensitive to UV light than normal keratinocytes are. When exposed at different concentrations before UV irradiation, nicotinamide seems to protect keratinocytes from multiple UV-induced damage, including oxidative stress, DNA impairments, and inflammation [9]. Studies in mice have shown that oral or topical application of nicotinamide prevents immunosuppression and reduces the number of UV-induced tumors. In humans, topical application of nicotinamide prevents UV-induced immunosuppression [8, 9]. Moreover, studies have demonstrated that niacinamide concentrations between 2% and 5% are effective in improving various skin conditions, including hyperpigmentation, fine lines, wrinkles, and skin barrier function [8, 9]. At 2%, effects of nicotinamide are present and have shown similar benefits to higher concentrations, decreasing the likelihood of skin irritation, redness, and itching, particularly in individuals with sensitive skin [10, 11].

The main objective of this study is to describe the morphological and molecular skin changes in photodamage and to assess the biological effects of a nicotinamide-containing broad-spectrum sunscreen (SSNP) in severely photodamaged skin. To achieve this objective, we used in vivo imaging with linear confocal optical coherence tomography (LC-OCT), immunohistochemistry (p53, PCNA, p21, and CPD), and RNA profiling.

METHODS

Patients and Samples

A total of 14 healthy subjects, 10 female and 4 male, mean age 52.6 years (range 41–66), were recruited in Hospital Clínic de Barcelona (Table 1).

Two areas of severely photodamaged forearm skin were identified (L01 and L02) and one less sun-damaged (naturally protected) area was identified on the inner part of the forearm (L03). An experienced dermatologist reviewed the skin and selected areas that were clearly photodamaged on the basis of the presence of fine wrinkles, xerosis, and lentiginosis.

All three areas were imaged using LC-OCT; two 3-mm punch biopsies were performed on L01 and L03 areas. As a result of technical problems, the L03 images of three patients were not obtained. A third biopsy was carried out after 4 weeks of the twice-daily application on an L02 area of a panthenol and nicotinamide-containing broad-spectrum sunscreen (SSNP) with a nicotinamide concentration of 2%. Each biopsy was split into two halves. The first half was fixed in formalin and paraffin embedded (FFPE) for hematoxylin and eosin and immunostaining with p21, p53, PCNA, and CPD. The other half was preserved in RNAlater (RNAprotect Tissue Reagent, Qiagen) and frozen to extract RNA and perform sequencing.

The study was approved in November 2019 by the Ethics Committee of Hospital Clínic de Barcelona, Spain (Nº HCB20190849). This study was performed in accordance with the ethical standards as laid down in the 1964 Declaration of Helsinki and its later amendments, or comparable ethical standards. The patients who took part in the study have given written informed consent to the publication of their case details.

Image Acquisition

Images were captured through LC-OCT (DAMAE Medical, Paris) based on an 800-nm-wavelength laser with axial resolution, lateral resolution and a field of view of 1.1–1.3 µm, and 1.2 $mm^2 \times 0.5$ mm^2 respectively. Images were captured at 350 µm [12]. LC-OCT images were analyzed using deep learning algorithms, as in previous publications [12]. The thickening of the stratum corneum, the epidermis thickness, the dermal–epidermal junction undulation, and keratinocyte quantification were evaluated through LC-OCT.

Scanned areas were compared to the first-half biopsy procedure utilizing hematoxylin and eosin (Supplementary material 1). Through hematoxylin and eosin standard histology, we evaluated the stratum spinosum (epidermis without stratum corneum), the dermal–epidermal junction undulation, and keratinocyte

quantification after imaging; one sample had a low-quality L03 image, and another had undefined L01 and L03 images. These inconveniences add to the previously explained lack of L03 samples from three patients.

Immunohistochemical Analysis

Immunohistochemical analysis was performed on 2-µm skin sections from FFPE samples. After 20-min antigen retrieval with citrate buffer (pH 6), samples were immunostained with p21, p53, PCNA, and CPD using a Leica Microsystems' Bond-max™ automated immunostainer together with a Bond Polymer Refine Detection System (Leica Microsystems). They were developed with diaminobenzidine and counterstained with hematoxylin. Control tissues for protocol optimization came from the Human Protein Atlas (IDIBAPS Biobank).

The immunohistochemical analysis compared biopsies stained with p21, p53, PCNA, and CPD pre and post 4-week treatment. Moreover, the number of positive and high-positive nuclei in 50 nuclei were counted. One of those samples did not have enough epidermis layer to conduct the immunohistochemical analysis, leaving the samples of 13 patients available for evaluation.

RNA Extraction and RNA Sequencing Analysis

Biopsies in RNAlater were frozen to extract RNA for sequencing. Total RNA was isolated from fresh tissue with Trizol, and purified with the RNeasy Minikit (Trizol-chloroform + RNeasy MinElute Cleanup Kit, Qiagen). RNA quantification was performed using a Qubit RNA BR Assay Kit. Integrity was measured by a Bioanalyzer RNA 6000 NanoKit (Agilent Technologies, Santa Clara, CA).

RNA samples were sent to the Centro Nacional de Análisis Genómico to conduct the stranded mRNA library preparation and sequencing on an HiSeq 4000 (Illumina).

RNA-Seq libraries were prepared from total RNA using a TruSeq Stranded mRNA LibraryPrep Kit (Illumina). mRNA was enriched with oligo-dT magnetic beads from the total RNA (500 ng) and fragmented to 80–450 nt. The second strand cDNA synthesis was performed in the presence of dUTP to achieve strand specificity. The blunt-ended double-stranded cDNA was 3′-adenylated and Illumina platform-compatible adaptors with unique dual indexes and unique molecular identifiers (Integrated DNA Technologies) were ligated. The ligation product was enriched with 15 PCR cycles. The final library was validated on a Bioanalyzer DNA 7500 assay. The libraries were sequenced on a NovaSeq6000 (Illumina) in paired-end mode with a read length of 2 × 101 bp, following the manufacturer's protocol for dual indexing. Image analysis, base calling ,and quality scoring of the run were processed using the manufacturer's software Real-Time Analysis (RTA 3.4.4) and followed by the generation of FASTQ sequence files. No incidences or quality problems occurred with the samples, allowing the analysis of the RNA sequencing from the 14 patients at three time points.

Table 1 Main characteristics of subjects included in the study

Volunteer	Age (years)	Phototype	Sex
P002	57	2	Male
P003	55	3	Male
P005	49	3	Female
P006	52	3	Female
P007	50	3	Female
P013	47	2	Male
P014	41	3	Female
P015	54	3	Female
P016	46	3	Female
P017	52	2	Female
P018	50	3	Male
P020	66	3	Female
P021	60	2	Female
P022	58	3	Female

Statistical Analysis

Student's *t* test was used to compare the mean of continuous variables that have a normal distribution. For non-normal variables, non-parametric statistics were used. The chi-squared test was used for contingency table comparison.

For histology and LC-OCT parameters, we compared L02 images before and after treatment, and L01 with L03 samples to examine the changes between severely photodamaged skin and less photodamaged skin. Additionally, we compared L01 with L02 samples to study the effect of SSNP treatment on photodamaged skin. All metrics were compared as paired data. The Wilcoxon signed-rank test and Spearman's correlation were applied. The linear regression was adjusted and p values < 0.05 were considered statistically significant.

For RNA-Seq data analysis, we correlated less sun-damaged samples (L03), photodamaged post-treatment samples (L02), and photodamaged pre-treatment samples (L01). Additionally, we compared L01 with L02 samples to study the effect of SSNP treatment on photodamaged skin.

R packages DearSeq and LIMMA were used for data normalization, specifically employing variance modeling at the observational level (VOOM). All analyses were paired for the patient and adjusted by sex. Genes with p value FDR < 0.05 were considered differential expressed genes (DEG). All analyses were performed using R version 3.3.0.

From the resultant DEGs, a pathway analysis was conducted using the hiPATHia tool (Babelomics). The "differential expression" option was chosen, and a patient-paired analysis performed. Pathways with p value < 0.05 were selected.

RESULTS

LC-OCT Results

The paired analysis of LC-OCT on L02 which was imaged before and after treatment in order to identify any possible effect did not show statistically significant differences: stratum corneum thickness 15 µm vs 14.46 µm, $p = 0.16$; stratum spinosum thickness 58.66 µm vs 55.6 µm, $p = 0.625$; dermoepidermal junction undulation 25.32% vs 21.43%, $p = 0.193$; keratinocyte layers 5.68 vs 5.10, $p = 0.375$.

The comparison of L01 and L02 after treatment samples also did not show significant differences (13 patients were evaluable; one had no good-quality L01 images).

We compared L01 with L03 samples in nine patients (three patients did not have an L03 image, one had a poor-quality L03 image, and one had undefined L01 and L03 images). L01 presents increased epidermal thickness (mean = 5.39 µm, $p = 0.0078$) and a higher number of keratinocytes per layer (mean = 0.997; $p = 0.002$). The volume of the different layers of keratinocytes seems greater for L01 (mean 0–20% = 4.61 μm^3, mean 40–60% = 26.22 μm^3, mean 80–100% = 55.34 μm^3). No differences are seen for the stratum corneum thickness and the dermoepidermal junction undulation.

Standard Histology

Compared to L01, L03 samples present an increased thickness of epidermis (mean = 11.07 µm, $p = 0.011$). Significantly higher keratinocyte layers are observed in L01 samples (mean = 0.77, $p = 0.029$).

In the analysis comparing L01 with L02, before and after treatment, there is no significant improvement in histological morphology defined parameters: the stratum spinosum, the dermal–epidermal junction undulation, and keratinocyte quantification.

Immunohistochemical Analysis

A total of 14 patients were included for evaluation. One of the samples had no epidermis layer, leaving only 13 which were evaluable.

At baseline, compared to less sun-damaged areas (L03), photodamaged skin (L01) presents a consistent increase in the expression of p21, PCNA, p53, and CPD.

To analyze the effect of 1-month treatment with SSNP, immunohistochemistry was

compared before and after treatment (L01–L02). p21 is the only marker showing a trend for decreased expression, with no statistical significance (Supplementary material 2).

Differential Gene Expression Analysis

A principal component analysis of genetic expression and a dendrogram shown graphically as a heatmap were derived tagging the three types of samples (Fig. 1).

The two graphs tend to separate pre-treated severely photodamaged skin from non-visibly sun-damaged skin samples. However, more diverse expression patterns are seen in post-treatment and non-visibly sun-damaged samples.

The gene differential expression study comparing L01, L02, and L03 samples show 1552 DEGs (Supplementary material 3).

The analysis comparing pre- and post-treatment photodamaged skin identifies 5429 DEGs, eight related to collagen, and they increased expression after treatment (Table 2).

Pathway Analysis from Significant Genes

The DEG pathway analysis shows MAPK and cGMP-PKG signalling pathways positively correlated with progression to photodamage and are higher in pre-treated photodamaged skin (Table 3).

In a pre- and post-treatment comparison, 32 pathways are downregulated after treatment, and five of them have a p value FDR < 0.1: ErbB, Hippo, NOD-like receptor, TNF, and NF-κB signalling pathways. Moreover, as in the progression to photodamage analysis, the MAPK signalling pathway was found to be significant (Table 3).

DISCUSSION

This study investigates morphological, histological, and molecular differences between severely photodamaged and less sun-damaged skin. It also studies biological changes induced by a panthenol and nicotinamide-containing broad-spectrum sunscreen (SSNP). It shows that there are gene expression differences when comparing severely photodamaged and less sun-damaged areas, improving knowledge of the pathophysiology of photodamaged skin. Moreover, data show that the use of SSNP can revert some of the negative effects of photodamage.

The morphological and histological studies reveal that non-visibly sun-damaged skin has fewer layers, that the dermal–epidermal junction is flatter in severely photodamaged areas, and that p21, PCNA, p53, and CPD are overexpressed in severely photodamaged skin. Concerning the dermal–epidermal junction flattening, our findings align with similar studies in the literature [13, 14].

The molecular pathways analysis shows that progression to photodamaged skin is associated with cGMP-PKG and MAPK signalling pathways. The cGMP-PKG signalling pathway mediates processes such as antivascular injury, anticardiac hypertrophy, and apoptosis inhibition. It has not previously been associated with photodamage or skin cancer, but it has been related to the proliferation, differentiation, and apoptosis of different cancer cells [15–19], and to an acceleration of metastasis in cervical cancer [20]. In this study, the cGMP-PKG signalling pathway is overexpressed in severely photodamaged skin. The MAPK signalling pathway is essential in cellular processes such as cell differentiation, division, and apoptosis. Its role in cancer and its relationship with photodamage has been demonstrated and is the target in treatments aiming at preventing it [6, 21, 22]. Studies show that oxidative stress plays a key role in triggering the MAPK pathway and that antioxidant agents can inactivate MAPK sub-pathways. The MAPK pathway is activated by UVB radiation and is responsible for the degradation of fibrillar type 1 collagen [5, 23], the most abundant in the dermal extracellular matrix. Also, activation of MAPK pathway causes inflammation and epidermal hyperplasia via the stimulated keratinocytes which, in response, will secrete pro-inflammatory cytokines such as IL-1, TNF, IL-6, and mediators including ICAM-1 and COX-2 [24].

The SSNP treatment shows modulation of 32 pathways implied in cell processes such as cell cycle, apoptosis, immune system, cell communication, cellular energy, or cancer.

The ErbB signalling pathway, which regulates the cell cycle, is downregulated after treatment with p value FDR < 0.1. Insufficient ErbB is associated with the development of neurodegenerative diseases, whereas excessive ErbB is associated with the development of solid tumors and is the target of some drugs for breast and colon cancer [25]. This pathway includes epidermal growth factor receptors, involved in photodamage and skin carcinogenesis [3]. Other pathways related to the cell cycle are Ras, Rap1, TGFβ, PI3K-Akt, VEGF, or MAPK signalling pathways. They are all related to UVB exposition [6] and have the ERK pathway in common, which is inhibited by nicotinamide [26]. This study shows that SSNP treatment downregulates cell cycle pathways and tempers the degradation of collagen activated by UVB irradiation in MAPK pathways.

In accordance with our results, a study in mice has shown that nicotinamide decreases the inflammatory response and apoptosis of sepsis in intestinal cells through Hippo signalling pathway regulation [27]. In our study, the Hippo signalling pathway is found with p value FDR < 0.1. This pathway plays a role in controlling organ size through the regulation of cell proliferation and apoptosis. The Hippo kinase cascade phosphorylates and inhibits the transcription co-activator "Yes-associated protein" and "transcriptional coactivator with PDZ-binding motif", resulting in their cytoplasmic retention and degradation.

Other pathways with p value FDR < 0.1 are related to the immune system: NOD-like receptors, NF-κB, and TNF signalling pathways. The combination of NOD-like receptors and their homologous agonists initiates a signalling cascade that leads to upstream regulation of NF-kB and the production of pro-inflammatory cytokines. In mouse experiments, the NOD-like receptor signalling pathway has been found to be inhibited by nicotinamide, in accordance with our results [28]. The TNF signalling pathway activates with UV and is able to induce fever, apoptotic cell death, cachexia, inflammation, inhibition of tumorigenesis and viral replication, and response to sepsis via IL-1 and IL-6 [6]. Additional pathways are related to the immune system, such as Toll-like receptor signalling, leukocyte transendothelial migration, Fc gamma R-mediated phagocytosis, or B cell receptor signalling pathways. The increase in immune response relates to photodamage through the promotion of ROS generation, proteolytic enzyme production, suppressed immune surveillance, and production of growth factors for incipient cancer cells [29].

Other significant pathways are activated by neuropeptides (GnRH, oxytocin, and neurotrophin signalling pathways). The neurotrophin signalling pathway has been associated with nicotinamide in animal experiments [30]. All these pathways activate MAPK signalling pathways, as reported in the literature.

Some pathways found are related to cellular energy (AMPK and FoxO signalling pathways) and cell communication (cAMP signalling, Gap junction, and focal adhesion pathways). Nicotinamide treatment has shown downregulation of the FOX pathway, reducing FoXo3 in human placenta [31] and downregulating AMPK and Camp pathways in cell experiments [27]. These pathways are regulators of other identified pathways. Specifically, AMPK and FoxO signalling pathways regulate the NF-kappa B signalling pathway [32, 33] and the PI3K-Akt signalling pathway [34, 35]. Additionally, cell communication pathways (cAMP signalling, Gap junction, and focal adhesion) also regulate the NF-kappa B signalling pathway [32, 36] and the PI3K-Akt signalling pathway [34, 37], as well as the cell cycle [38, 39]. This study shows that they are downregulated after SSNP treatment.

Finally, significant pathways directly related to cancer (Proteoglycans in cancer, Choline metabolism in cancer, Pathways in cancer, and Wnt signalling pathway) are downregulated after treatment, suggesting photodamage as an intermediate stage between healthy skin and cancer.

Additionally, after treatment, eight genes related to collagen I, III, VI, XII, XVI, and XXI are overexpressed.

In imaging techniques, no statistically significant pre- and post-treatment differences are found. The small number of samples analyzed

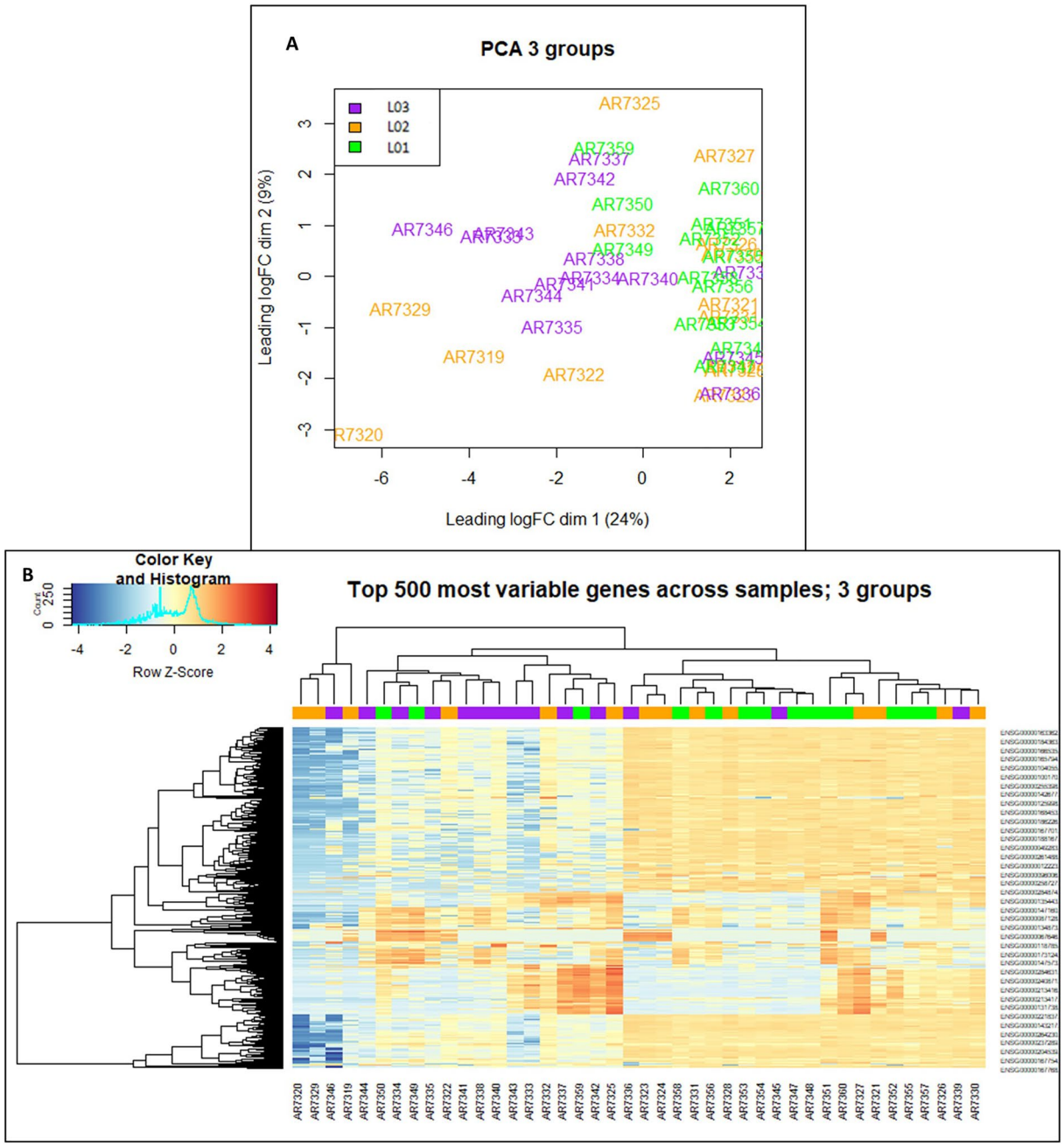

Fig. 1 Principal component analysis (**a**) and heatmap (**b**) of photodamage analysis from less sun-damaged to pre-treated photodamaged skin. *L03* less sun-damaged samples, *L02* photodamaged post-treatment samples, *L01* photodamaged pre-treatment samples

Table 2 Expression level of DEGs related to collagen in the analysis comparing pre and post SSNP-treated samples

	L01	L02
COL16A1	1023.29	2391.64
COL1A1	7462.21	86,971.93
COL1A2	25,345.29	142,289.43
COL21A1	177.71	405.64
COL3A1	16,392.43	104,431.00
COL4A5	456.93	895.29
COL4A6	206.21	320.00
COL6A1	1974.71	4118.07
Mean	6629.85	42,727.88

L02 photodamaged post-treatment samples, *L01* photodamaged pre-treatment samples, *DEGs* differentially expressed genes, *SSNP* panthenol and nicotinamide-containing broad-spectrum sunscreen

by LC-OCT together with the brief 4-week treatment duration limits the observation of morphological changes, diluting the effect on the four patients who showed changes.

The primary limitation of this work is the absence of a vehicle arm to compare the effects of the niacinamide-containing sunscreen with a sunscreen formulation lacking niacinamide. This omission prevents us from attributing the observed results solely to niacinamide, as the comparative effects of the base sunscreen were not independently assessed. Additionally, the small sample size of 14 subjects limits the generalizability of the findings. The treatment duration of 4 weeks may be insufficient to observe significant morphological changes, suggesting that longer treatment periods might yield more substantial results. Ethical and practical constraints limited the number of invasive biopsies, restricting the tissue available for analysis. These limitations highlight the need for more comprehensive studies with larger sample sizes and longer durations, to fully understand the effects of niacinamide-containing sunscreens on photodamaged skin.

CONCLUSION

Our results present cGMP-PKG and MAPK signalling pathways as crucial in photodamage. The MAPK signalling pathway and others implied in the cell cycle, apoptosis processes, and immune system are downregulated after SSNP treatment, thus confirming the efficacy of this treatment. The study also suggests a role of SSNP in the increase of collagen production.

Table 3 Pathway analysis from significant genes (*p* value FDR < 0.05) in the progression of photodamage analysis and in the analysis comparing pre and post SSNP-treated samples

Progression of photodamage analysis		
Path	**UP/DOWN (From L03 to L01)**	***p* value**
MAPK signalling pathway	UP	4.44E−02
cGMP-PKG signalling pathway	UP	4.44E−02
Analysis comparing pre and post SSNP-treated samples		
Path	**UP/DOWN (L01 to L02)**	***p* value**
ErbB signalling pathway	DOWN	6.10E−04 (FDR 5.42E−02)
Hippo signalling pathway	DOWN	8.54E−04 (FDR 5.42E−02)
NOD-like receptor signalling pathway	DOWN	8.54E−04 (FDR 5.42E−02)
TNF signalling pathway	DOWN	8.54E−04 (FDR 5.42E−02
NF-kappa B signalling pathway	DOWN	1.71E−03 (FDR 9.63E−02)
AMPK signalling pathway	DOWN	1.07E−02
Cell cycle	DOWN	1.07E−02
Fc gamma R-mediated phagocytosis	DOWN	8.54E−03
Neurotrophin signalling pathway	DOWN	1.34E−02
Proteoglycans in cancer	DOWN	5.25E−03
Ras signalling pathway	DOWN	1.34E−02
Toll-like receptor signalling pathway	DOWN	8.54E−03
Leukocyte transendothelial migration	DOWN	1.66E−02
Rap1 signalling pathway	DOWN	1.66E−02
TGF-beta signalling pathway	DOWN	2.02E−02
cAMP signalling pathway	DOWN	2.45E−02
Choline metabolism in cancer	DOWN	2.45E−02
Focal adhesion	DOWN	2.45E−02
FoxO signalling pathway	DOWN	2.45E−02
GnRH signalling pathway	DOWN	2.45E−02
Hedgehog signalling pathway	DOWN	2.45E−02
MAPK signalling pathway	DOWN	2.45E−02
Oxytocin signalling pathway	DOWN	2.45E−02

Table 3 continued

Analysis comparing pre and post SSNP-treated samples		
Path	**UP/DOWN (L01 to L02)**	***p* value**
Pathways in cancer	DOWN	2.45E−02
Wnt signalling pathway	DOWN	2.53E−02
B cell receptor signalling pathway	DOWN	2.95E−02
Natural killer cell mediated cytotoxicity	DOWN	2.95E−02
RIG-I-like receptor signalling pathway	DOWN	2.95E−02
T cell receptor signalling pathway	DOWN	2.95E−02
VEGF signalling pathway	DOWN	2.95E−02
Gap junction	DOWN	4.19E−02
PI3K-Akt signalling pathway	DOWN	4.94E−02

Source: Hipathia tool

L03 less sun-damaged samples, *L02* photodamaged post-treatment samples, *L01* photodamaged pre-treatment samples, *SSNP* panthenol and nicotinamide-containing broad-spectrum sunscreen

ACKNOWLEDGEMENTS

Thanks to all subjects included, who are the main reason for our studies; to nurses from the Melanoma Unit of Hospital Clínic of Barcelona and to the Biobank core facility of Institut d'Investigacions Biomèdiques August Pi i Sunyer (IDIBAPS) for the technical help. Paul Hetherington provided a thorough review and made significant improvements to the language and writing of the draft manuscript.

Author Contributions. Susana Puig, Míriam Potrony, and Gemma Tell-Martí conceived the idea presented in this study. Carmen Orte Cano, Elisa Cinotti, Véronique Del Marmol, Margot Fontaine, Makiko Miyamoto, Jilliana Monnier, Jean Luc Perrot, Pietro Rubegni, Linda Tognetti, Josep Malvehy, and Susana Puig provided the clinical perspective for the idea. Anne Laure Demessant-Flavigny, Caroline Le Floc, and Leonor Prieto contributed extensive knowledge about nicotinamide-containing broad-spectrum sunscreens and facilitated their acquisition. Pablo Iglesias and Susana Puig managed patient recruitment and visits. Pablo Iglesias, Josep Malvehy, and Susana Puig conducted consultations with the patients included. Javiera Pérez-Anker and Beatriz Alejo acquired the LC-OCT images. Javiera Pérez-Anker and Pau Rosés-Gibert interpreted the LC-OCT results. Natalia Espinosa conducted the immunohistochemical analyses. Pau Rosés-Gibert and Natalia Espinosa interpreted the immunohistochemistry results. Mariano Suppa, Anne Laure Demessant-Flavigny, Judit Mateu, Gemma Tell-Martí, and Neus Calbet-Llopart organized and oversaw RNA extraction, as well as the shipment of samples to the Centro Nacional de Análisis Genómico. Teresa Torres-Moral, Gemma Tell-Martí, and Jaume Bague conducted the bioinformatic analysis related to RNA-sequencing. Teresa Torres-Moral, Jaume Bague, and Gemma Tell-Martí collaborated on the interpretation of RNA sequencing results. Teresa Torres-Moral, Pau Rosés-Gibert, Javiera Pérez-Anker, and Susana Puig provided interpretation of the overall results. Teresa Torres-Moral drafted the initial manuscript. Susana Puig supervised the findings of this work. All authors participated in result discussions and contributed to the final manuscript.

Funding. L'Oréal/La Roche-Posay funded the study, publication cost and the journal's Rapid Service Fee.

Data Availability. Due to the sensitivity of the molecular data analyzed, they have not been shared.

Declarations

Conflict of Interest. All authors declare some conflict of interest since La Roche-Posay funded this study. Moreover, Anne Laure Demessant-Flavigny, Leonor Prieto and Caroline Le Floc'h are L'Oreal Employees. In the last 36 months, existing conflict of interests were: Véronique Del Marmol have grants or contracts from BMS, MSD, Almirall and Sanofia; Josep Malvehy and Susana Puig from Abbvie, Almirall, Amgen, BMS, Biofrontera, Canfield, Cantabria, Fotofinder, GSK, ISDIN, La Roche Posay, Leo Pharma, MSD, MEDA, Novartis, Polychem, Roche and Sun Pharma. Véronique Del Marmol has received consulting fees from BMS, MSD, Sanofi, Merck, Almirall, Abbvie, Leo pharma, Pierre fabre, andNovartis. Josep Malvehy and Susana Puig have received payment or honoraria for lectures, presentations, speaker bureaus, manuscript writing or educational events from Roche Posay, Pierre-Fabre, Almirall and ISDIN; Jilliana Monnier from BMS, Pierre Fabre and Novartis; MP from ISDIN; Véronique Del Marmol from BMS, MSD,Sanofi, Sun pharma, Pierre fabre and Novartis. Josep Malvehy and Susana Puig received support for attending meetings and/or travel from Roche Posay, Pierre-Fabre, Almirall and ISDIN; Véronique Del Marmol from BMS, MSD, Pierre Fabre and Novartis; Josep Malvehy and Susana Puig participated on a Data Safety Monitoring Board Advisory Board for Pierre-Fabre, Almirall, SunPharma. Josep Malvehy and Susana Puig have stock options in Athena Tech of Dermavision.

Ethical Approval. The study was approved in November 2019 by the Ethics Committee of Hospital Clínic de Barcelona, Spain (Nº HCB20190849). This study was performed in accordance with the ethical standards as laid down in the 1964 Declaration of Helsinki and its later amendments or comparable ethical standards. The patients who took part in the study have given written informed consent to the publication of their case details.

REFERENCES

1. Lin TY, Wu PY, Hou CW, et al. Protective effects of sesamin against UVB-induced skin inflammation and photodamage in vitro and in vivo. Biomolecules. 2019. https://doi.org/10.3390/biom9090479.

2. Solano F. Photoprotection and skin pigmentation: melanin-related molecules and some other new agents obtained from natural sources. Molecules. 2020. https://doi.org/10.3390/molecules25071537.

3. Ha SJ, Lee J, Park J, et al. Syringic acid prevents skin carcinogenesis via regulation of NoX and EGFR signaling. Biochem Pharmacol. 2018;154:435–45.

4. Han H. Nonnegative principal component analysis for mass spectral serum profiles and biomarker discovery. BMC Bioinform. 2010;11:S1–S1.

5. Kondo S. The roles of cytokines in photoaging. J Dermatol Sci. 2000;23(Suppl 1):S30–6.

6. Han SH, Ballinger E, Choung SY, et al. Anti-photoaging effect of hydrolysates from pacific whiting

skin via MAPK/AP-1, NF-κB, TGF-β/Smad, and Nrf-2/HO-1 signaling pathway in UVB-induced human dermal fibroblasts. Mar Drugs. 2022. https://doi.org/10.3390/md20050308.

7. Surjana D, Halliday GM, Damian DL. Role of nicotinamide in DNA damage, mutagenesis, and DNA repair. J Nucleic Acids. 2010;2010:157591.

8. Snaidr VA, Damian DL, Halliday GM. Nicotinamide for photoprotection and skin cancer chemoprevention: a review of efficacy and safety. Exp Dermatol. 2019;28:15–22. https://doi.org/10.1111/exd.13819.

9. Camillo L, Gironi LC, Zavattaro E, Esposto E, Savoia P. Nicotinamide attenuates UV-induced stress damage in human primary keratinocytes from cancerization fields. J Invest Dermatol. 2022;142(5):1466–77.e1. https://doi.org/10.1016/j.jid.2021.10.012.

10. Ong R, Goh C. Niacinamide: a review on dermal delivery strategies and clinical evidence. Drug Deliv Transl Res. 2024. https://doi.org/10.1007/s13346-024-01028-7.

11. Draelos ZD, Matsubara A, Smiles K. The effect of 2% niacinamide on facial sebum production. J Cosmet Laser Ther. 2006;8(2):96–101. https://doi.org/10.1080/14764170600717704.

12. Fischman S, Pérez-Anker J, Tognetti L, et al. Non-invasive scoring of cellular atypia in keratinocyte cancers in 3D LC-OCT images using deep learning. Sci Rep. 2022. https://doi.org/10.1038/s41598-021-04395-1.

13. Freeman RG, Cockerell EG, Armstrong JT, et al. Sunlight as a factor influencing the thickness of epidermis. J Invest Dermatol. 1962;39:295–8.

14. Amano S. Characterization and mechanisms of photoageing-related changes in skin. Damages of basement membrane and dermal structures. Exp Dermatol. 2016;25:14–9.

15. Ren Y, Zheng J, Yao X, et al. Essential role of the cGMP/PKG signaling pathway in regulating the proliferation and survival of human renal carcinoma cells. Int J Mol Med. 2014;34:1430–8.

16. Ren Y, Feng X, Xia X, et al. Gender specificity improves the early-stage detection of clear cell renal cell carcinoma based on methylomic biomarkers. Biomark Med. 2018;12:607–18.

17. Fajardo AM, Piazza GA, Tinsley HN. The role of cyclic nucleotide signaling pathways in cancer: targets for prevention and treatment. Cancers (Basel). 2014;6:436–58. https://doi.org/10.3390/cancers6010436.

18. Schwappacher R, Rangaswami H, Su-Yuo J, et al. cGMP-dependent protein kinase Iβ regulates breast cancer cell migration and invasion via interaction with the actin/myosin-associated protein caldesmon. J Cell Sci. 2013;126:1626–36.

19. Kong X, Wang JS, Yang H. Upregulation of lncRNA DARS-AS1 accelerates tumor malignancy in cervical cancer by activating cGMP-PKG pathway. J Biochem Mol Toxicol. 2021;35:1–11.

20. Gong L, Lei Y, Tan X, et al. Propranolol selectively inhibits cervical cancer cell growth by suppressing the cGMP/PKG pathway. Biomed Pharmacother. 2019;111:1243–8.

21. Muthusamy V, Piva TJ. The UV response of the skin: a review of the MAPK, NFκB and TNFα signal transduction pathways. Arch Dermatol Res. 2010;302:5–17. https://doi.org/10.1007/s00403-009-0994-y.

22. Rittié L, Fisher GJ. UV-light-induced signal cascades and skin aging. Aging. 2002;1(4):705–20.

23. Rodríguez-Rojas F, Celis-Plá PSM, Méndez L, et al. MAPK pathway under chronic copper excess in green macroalgae (Chlorophyta): involvement in the regulation of detoxification mechanisms. Int J Mol Sci. 2019;20:4546.

24. Ansel J, Perry P, Brown J, et al. Cytokine modulation of keratinocyte cytokines. J Investig Dermatol. 1990;94:s101–7.

25. Hynes NE, MacDonald G. ErbB receptors and signaling pathways in cancer. Curr Opin Cell Biol. 2009;21:177–84.

26. Song X, Xu A, Pan W, et al. Nicotinamide attenuates aquaporin 3 overexpression induced by retinoic acid through inhibition of EGFR/ERK in cultured human skin keratinocytes. Int J Mol Med. 2008;22:229–36.

27. Kuang Z-S, Leng Y-X, Yang N, et al. Inhibition of visfatin alleviates sepsis-induced intestinal damage by inhibiting Hippo signaling pathway. Inflamm Res. 2022. https://doi.org/10.1007/s00011-022-01593-z.

28. Wang X, Li B, Liu L, et al. Nicotinamide adenine dinucleotide treatment alleviates the symptoms of experimental autoimmune encephalomyelitis by activating autophagy and inhibiting the NLRP3 inflammasome. Int Immunopharmacol. 2021. https://doi.org/10.1016/j.intimp.2020.107092.

29. Bennett MF, Robinson MK, Baron ED, et al. Skin immune systems and inflammation: protector of the skin or promoter of aging? J Investig Dermatol

Sympos Proc. 2008. https://doi.org/10.1038/jidsymp.2008.3.

30. Kuchmerovs'ka TM. Neurotrophic action of nicotinamide and nicotinoyl-GABA in rat brain in experimental Parkinsonism. Ukr Biokhim Zh (1978). 1998;70:126–31.

31. Lappas M, Permezel M. The anti-inflammatory and antioxidative effects of nicotinamide, a vitamin B3 derivative, are elicited by $FoxO_3$ in human gestational tissues: Implications for preterm birth. J Nutr Biochem. 2011;22:1195–201.

32. Parry GC, Mackman N. Role of cyclic AMP response element-binding protein in cyclic AMP inhibition of NF-κB-mediated transcription. J Immunol. 1997;159(11):5450–6.

33. Salminen A, Hyttinen JM, Kaarniranta K. AMP-activated protein kinase inhibits NF-κB signaling and inflammation: impact on healthspan and lifespan. J Mol Med (Berl). 2011;89(7):667–76.

34. Sato N, Sato K, Kudo M, et al. Activation of phosphatidylinositol 3-kinase by cAMP-dependent protein kinase in normal human melanocytes. J Invest Dermatol. 1996;107(1):97–102.

35. Gwinn DM, Shackelford DB, Egan DF, et al. AMPK phosphorylation of raptor mediates a metabolic checkpoint. Mol Cell. 2008;30(2):214–26.

36. Mendoza-Naranjo A, Cormie P, Serrano AE, et al. Targeting gap junctions in tumor cells to inhibit metastasis. J Cell Biol. 2011;192(5):789–805.

37. King WG, Mattaliano MD, Chan TO, et al. Phosphatidylinositol 3-kinase is required for integrin-stimulated AKT and Raf-1/mitogen-activated protein kinase pathway activation. Mol Cell Biol. 1997;17(8):4406–18.

38. Goodenough DA, Paul DL. Gap junctions. Cold Spring Harb Perspect Biol. 2009;1(1):a002576.

39. Assoian RK, Schwartz MA. Coordinate signaling by integrins and receptor tyrosine kinases in the regulation of G1 phase cell-cycle progression. Curr Opin Genet Dev. 2001;11(1):48–53.